THE JOURNAL OF PHYSICAL CHEMISTRY B

Article

pubs.acs.org/JPCB

# Coarse-Grained Modeling of the Titration and Conductance Behavior of Aqueous Fullerene Hexa Malonic Acid (FHMA) Solutions

Stuart A. Allison,* Hengfu Wu, Avery Moyher, Linda Soegiarto, Bi Truong, Duy Nguyen, Tam Nguyen, and Donghyun Park

Department of Chemistry, Georgia State University, Atlanta, Georgia 30302-3965, United States

Supporting Information

**ABSTRACT:** The coarse-grained continuum primitive model is developed and used to characterize the titration and electrical conductance behavior of aqueous solutions of fullerene hexa malonic acid (FHMA). The spherical FHMA molecule, a highly charged electrolyte with an absolute valence charge as large as 12, is modeled as a dielectric sphere in Newtonian fluid, and electrostatics are treated numerically at the level of the non-linear Poisson−Boltzmann equation. Transport properties (electrophoretic mobilities and conductances) of the various charge states of FHMA are numerically computed using established numerical algorithms. For reasonable choices of the model parameters, good agreement between experiment (published literature) and modeling is achieved. In order to accomplish this, however, a moderate degree of specific binding of principal counterion and FHMA must be included in the modeling. It should be emphasized, however, that alternative explanations are possible. This comparison is made at 25 °C for both $Na^+$ and $Ca^{2+}$ principal counterions. The model is also used to characterize the different charge states and degree of counterion binding to those charge states as a function of pH.

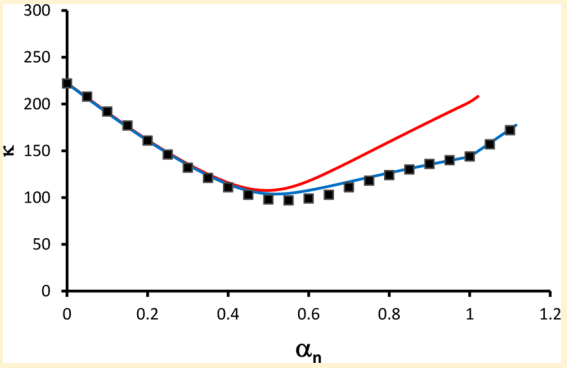


## 1. INTRODUCTION

Conductance measurements of aqueous solutions containing ionic species are comparatively simple to carry out and are capable of providing valuable information about ions and their interaction with solvent.[1] One of the early successes of continuum modeling of transport concerned the electrical conductance of dilute aqueous solutions of strong electrolytes.[2−4] Initially limited to very dilute solutions of ions modeled as point charges, the theory was subsequently extended to higher concentrations, and generalized to account, to lowest order, for the finite size of the ions of arbitrary valence.[5−13] Recently, progress has been made in extending this theoretical modeling strategy to highly charged nanoparticles,[14] and it is an application of this approach that is the focus of the present study.

Since its discovery in 1985,[15] Buckminsterfullerene, $C_{60}$, has stimulated great interest due to its possible applications in biomedicine,[16,17] electronics,[18] and optics.[19] The fundamental structure of $C_{60}$ is well characterized,[20] and in benzene, it has a hydrodynamic radius of 0.41 nm, which comes from measurement of its self-diffusion constant by $^{13}C$ pulsed-field gradient NMR.[21] The poor water solubility of $C_{60}$ can be dealt with by attaching hydrophilic side groups to its surface as is done in the case of fullerene hexa malonic acid, FHMA, $C_{60}(C(COOH)_2)_6$.[22] An atomic model of FHMA is shown in Figure 1. The development of water-soluble fullerene derivatives is essential in their applications to biological systems.

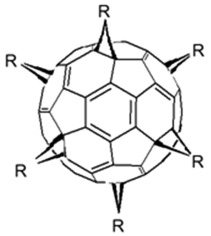


**Figure 1.** Structure of FHMA. FHMA contains six malonic acid substituents ($C(COOH)_2$) covalently attached to the $C_{60}$ fullerene core. Partial deprotonation of FHMA renders it water-soluble. The radius of the fullerene core is 0.35 nm.[20]

Physico-chemical studies of FHMA have been carried out[22−24] and these are important for a number of reasons. FHMA nanoparticles are comparatively small and have simple, symmetric structures that make them ideal for model studies. At the same time, they are highly charged and can be regarded as prototypical polyelectrolytes. However, this high charge as well the variability in the degree of deprotonation/charge presents challenges from the standpoint of modeling. On a theoretical level, the free solution electrophoretic mobility of

**Received:** January 7, 2014
**Revised:** February 24, 2014
**Published:** February 26, 2014

charged spherical particles modeled within the framework of the continuum primitive model is well established.[25−29] Once the electrophoretic mobilities of the charged species comprising an aqueous solution are known, it is also straightforward to compute the electrical conductivity of model solutions.[14] In addition to the mobility of the different possible FHMA species, however, we also need to know their concentrations.

The primary objective of the present work is to carry out a detailed modeling study of the pH titration and conductance behavior of FHMA particles within the framework of the continuum primitive model and compare the model studies with experiment.[22−24] This modeling is coarse grained. The FHMA particle is modeled as a sphere with hydrodynamic radius a with a centrosymmetric charge distribution that arises from deprotonation of malonic acid groups on its surface. These fixed charges are assumed to reside at distance $b$ from the center of the sphere. The surrounding media is modeled as a continuum Newtonian fluid. The ion atmosphere arising from the presence of small ions ($H^+$, $OH^-$, and cation $A^{+z}$), and the various charge states resulting from variable deprotonation of FHMA is treated as a continuum in determining the electrostatic potential around the different charged states of the model FHMA. This involves numerical solution of the non linear Poisson−Boltzmann equation for all possible charge states of the "host" model FHMA particle. The fixed charge is assumed to reside at a fixed distance from the center of the host particle. Also, other (FHMA) particles can contribute to the ionic environment of the host particle, but cannot approach the host within a distance of twice the hydrodynamic radius. Account shall also be taken of specific cation binding to the more highly deprotonated particle forms. Electrophoretic mobilities of the different charge states of FHMA are numerically computed using the O'Brien−White procedure.[29] As discussed in the Supporting Information, the electrophoretic mobilities of $H^+$, $OH^-$, and $A^{+z}$ are computed using a "small ion" model. The total solution conductance is related in a simple way to the concentrations and mobilities of all ions present. This methodology is applied to the titration and conductance behavior of FHMA aqueous solutions counterion $Na^+$ and to a more limited extent $Ca^{2+}$. In the present work, it is necessary to include specific counterion binding of both $Na^+$ and $Ca^{2+}$ in order to obtain good agreement between modeling and experiment.[22−24] We would like to emphasize, however, that specific counterion binding is only one possible explanation for the observed conductance behavior. We shall return to this point at the end of this work. Since modeling also requires knowledge of the concentrations of deprotonated FHMA species as well as specifically bound counterion−FHMA complexes, we also examine these distributions.

## 2. METHODS

The particle is modeled as a sphere with hydrodynamic radius a containing a centro-symmetric fixed charge distribution located at distance $b$ ($b \geq a$) from the distance of the sphere. This charge arises from the deprotonation of an even number, $n$, of titratable proton sites. It is assumed that there are two distinct classes of sites with intrinsic acid dissociation constants, $K_1$ and $K_2$. In the case of FHMA, these sites correspond to six malonic acid groups, $C(COOH)_2$, covalently attached to the fullerence core. We start with $c_x = c/n$ mol/liter of FHMA particles in a water solvent at temperature $T$ at initial pH equal to $pH_0$. The initial solution will be fairly acidic resulting from (partial) deprotonation of FHMA. This solution is titrated with concentrated base, $A(OH)_z$ where A is the cation (valence charge z). As base is added to the solution, $OH^-$ from the base combines with $H^+$ and the pH rises. Define $\alpha_n$ as the moles of added $A(OH)_z/(zc)$ so that the beginning of the titration correspond to $\alpha_n = 0$ and $\alpha_n = 1$ corresponds to adding just enough base to neutralize all of the titration sites of FHMA. In order to account for the conductance, $\kappa$, observed experimentally, it is necessary to include specific binding $A^{+z}$ to (partially) deprotonated states FHMA. We introduce an intrinsic binding constant, $K_B$, to account for this and binding of A shall only be considered to occur to doubly deprotonated groups (over half of the titratable sites of FHMA are deprotonated). In order to calculate the titration profile, $\alpha_n$ versus pH, of FHMA, we need to determine the concentration of the various deprotonated species, $[XH_{n-j}]$ ($j$ ranges from 0 to $n$), as well as the concentration of the various cation bound complexes, $[XH_{n-j}A_k]$ with as few input parameters as possible. The details of the modeling procedure both with regard to the calculation of the concentration of the various FHMA species as well as the conductance are placed in the Supporting Information file since this is important, but of interest to a limited audience. To summarize, input parameters to determine the titration curve include $pK_1$, $pK_2$, $pK_B$, $a$, $b$, $T$, $c_x$, and the relative permittivity of the solvent, $\varepsilon_r$. As discussed at some length in the Supporting Information, account is taken of multiple configurations as well as how the charge state and ionic screening influence deprotonation/binding. One requirement is knowledge of the electrostatic potential in the vicinity of the model FHMA for all possible charge states, and this requires an iterative numerical procedure to solve the non linear Poisson−Boltzmann equation.[14] In order to calculate the conductivity, $\kappa$, "small ion" theory is[1−13] is used to compute the contribution of $H^+$, $OH^-$, and $A^{+z}$; and the O'Brien−White procedure[29] is used to calculate the contribution of the various FHMA states as discussed in the Supporting Information.

The hydrodynamic radius of $C_{60}$ in benzene has been measured to be 0.41 nm,[21] but the presence of six malonic acid groups, $(C(COOH)_2)$, attached to the core sphere is expected to result in a substantially larger hydrodynamic radius for FHMA. As far as we are aware, however, there have been no direct measurements of $a$ from diffusion measurements by NMR[21] or boundary spreading techniques.[30] A value of 0.77 nm has been used for FHMA, but this is based on an analysis of density data, not transport.[22] We shall estimate a for FHMA using the "volume increment" method of Edward.[31] Assuming a core radius of 0.4 nm, we then add the appropriate volume increments tabulated in ref 31 for six malonic acid groups. A simple calculation yields a volume corresponding to a sphere of 0.6 nm in radius. In "Model A", we shall set $a = b$ (the distance of fixed charges from the center of the sphere) equal to 0.6 nm. To illustrate the sensitivity of the results on $a$ (and $b$), we shall also consider two other models which correspond to smaller (Model B: $a = 0.45$ nm, $b = 0.60$ nm), and larger (Model C: $a = b = 0.77$ nm) model FHMA particles than Model A. We shall ignore the variation of a with state of deprotonation or binding of $A^{+z}$ ions. The particle size, on the basis of $a$, increases in the order Model B, Model A, Model C.

## 3. RESULTS

**3.1. $pK_1$ and $pK_2$ for Models A, B, and C (No Counterion Binding).** The most straightforward way of determining $pK_1$ and $pK_2$ for our FHMA models is to adjust them until a good match is obtained between expermimental


dx.doi.org/10.1021/jp500196j | J. Phys. Chem. B 2014, 118, 3150−3155

titration (pH versus $\alpha_n$) and conductance ($\kappa$ versus $\alpha_n$) behavior and modeling. For the moment, we shall not consider counterion binding and will set $pK_B = +5$, which insures this condition. We shall analyze the titration data of FHMA with NaOH at 25 °C reported by Cerar et al.[22] The concentration of FHMA, $c_x$, is $1.15 \times 10^{-4}$ M. At the beginning of the titration ($\alpha_n = 0.0$), the pH is expected to depend primarily on the dissociation of most acidic protons of FHMA, or $pK_1$. In addition, the conductance at the beginning of the titration is expected to be very sensitive to $pK_1$ as well. The way the program is structured, the pH is read in as an input parameter (along with $pK_1$, $pK_2$, $pK_B$, and a number of other parameters) and $\alpha_n$ is calculated (eq 20 in the Supporting Information).

The pH corresponding to $\alpha_n = 0$, $pH_0$, can be determined by testing a range of initial pH values, determining their corresponding $\alpha_n$ values, and then interpolating what pH value yields $\alpha_n = 0$. It turns out that the initial pH is fairly insensitive to $pK_1$, but the conductivity, $\kappa$, is quite sensitive to $pK_1$. Consequently, the $\kappa$ value corresponding to $\alpha_n = 0$ is also useful in matching experimental and model data for $\alpha_n = 0$. From experiment $pH_0$ is about 3.25 and $\kappa$ equals 222 (in $10^{-4}$ $\Omega^{-1}$ $m^{-1}$). The appropriate $pK_2$ value can be determined by matching the experimental and model titration curves in the range $0.5 < \alpha_n < 1.0$. Good model fits to experimental titration curves for Models A, B, and C assuming no binding of $Na^+$ can be found by suitable adjustment of $pK_1$ and $pK_2$. However, if we compare the corresponding model conductivity, $\kappa$ (in $10^{-4}$ $1/(\Omega$ m)), versus $\alpha_n$ behavior with experiment, substantial differences are apparent as shown in Figure 2. For $\alpha_n$ less than about 0.2, model and experimental $\kappa$ values are in excellent agreement, but at higher $\alpha_n$, model conductivities exceed experiment. However, better agreement with experiment is achieved by choosing larger a values (Models A and C). We interpret the discrepancy between model and experiment at large $\alpha_n$ to be indicative of specific binding of $Na^+$ to fullerene that goes above and beyond simple electrostatic interactions between the deprotonated carboxylic acid sites of FHMA and the principle counterion, $Na^+$. In the next subsection, we shall address this question for Models A and C. We shall not pursue Model B any further since a is too small on structural grounds to be realistic. It has been included here simply to illustrate how it is possible to fit the titration curve for a broad range of particle sizes by appropriate adjustment of just two parameters, $pK_1$ and $pK_2$.

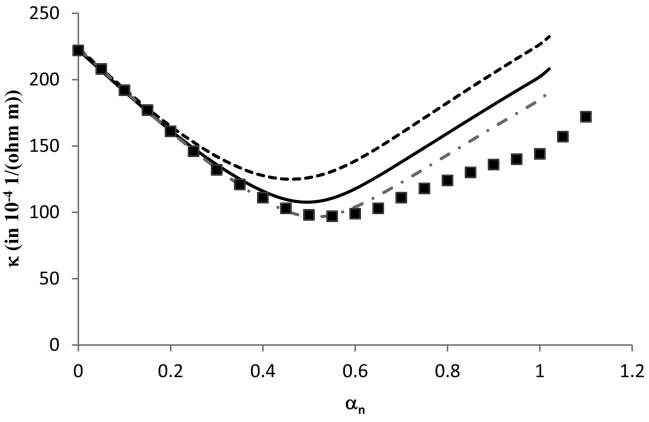


**Figure 2.** Conductivity, $\kappa$ (in $10^{-4}$ $1/(\Omega$ m)), versus $\alpha_n$ of FHMA and Models A, B, and C with no counterion binding at 25 °C, $c_x = 1.15 \times 10^{-4}$ M. Squares represent experimental values and darked dashed, solid, and light dashed lines correspond to Models A, B, and C, respectively. See the text for details regarding the values of $pK_1$ and $pK_2$ appropriate for each model ($pK_B = +5.0$).

**3.2. Inclusion of $Na^+$ Specific Binding for Models A and C.** Call the procedure outlined in Section 3.1 to obtain $pK_1$ and an initial estimate $pK_2$ "Step 1". To account for the possibility of counterion binding, set $pK_1$ and $pK_2$ to the values obtained in Step 1 and consider a range of $pK_B$ values and attempt to match model and experimental $\kappa$, and this is called "Step 2". A complicating feature of the model is that counterion binding, holding $pK_2$ constant, induces the release of protons at large $\alpha_n$. In other words, the titration curve is influenced by $pK_B$ as well as $pK_1$ and $pK_2$. Once a $pK_B$ value is found that matches the experimental $\kappa$ versus $\alpha_n$ curve, it is necessary to make further adjustments in $pK_2$ (call this "Step 3") to match model and experimental titration curves. It may be possible to iterate Steps 2 and 3 to obtain ultimate convergence. The results of this procedure applied to Model A are shown in Figures 3 and 4. In these figures, the optimal parameters for $pK_1$, $pK_2$, and $pK_B$ are 1.8, 4.2, and −1.4, respectively. A similar analysis

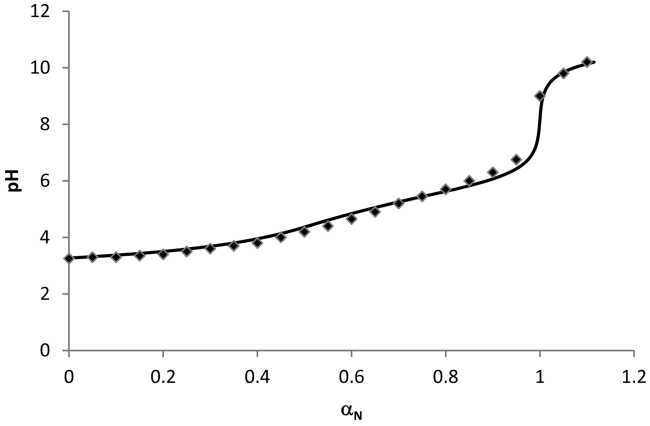


**Figure 3.** Titration curve (pH versus $\alpha_n$) of FHMA and Model A with $pK_1 = 1{,}8$, $pK_2 = 4.2$, and $pK_B = -1.4$ at 25 °C, $c_x = 1.15 \times 10^{-4}$ M. Squares represent experimental values and the solid line the corresponding model values.

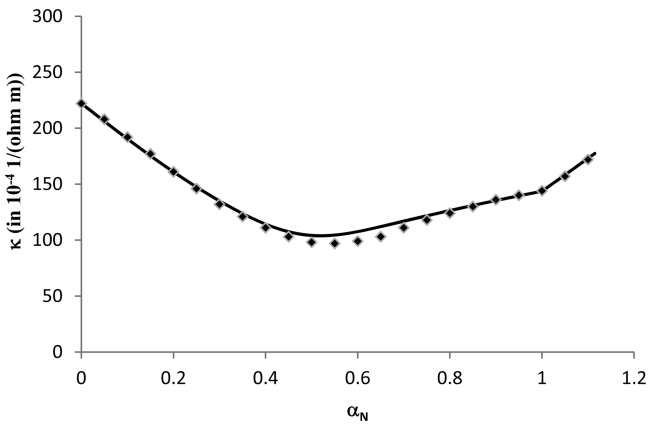


**Figure 4.** Conductivity, $\kappa$ (in $10^{-4}$ $1/(\Omega$ m)), versus $\alpha_n$ of FHMA and Model A with $pK_1 = 1{,}8$, $pK_2 = 4.2$, and $pK_B = -1.4$ at 25 °C, $c_x = 1.15 \times 10^{-4}$ M. Squares represent experimental values and the solid line the corresponding model values.


dx.doi.org/10.1021/jp500196j | J. Phys. Chem. B 2014, 118, 3150−3155

applied to Model C leads to optimal parameters for $pK_1$, $pK_2$, and $pK_B$ yields 1.9, 4.5, and −1.5.

**3.3. Conductance of FHMA in the Presence of $Ca^{2+}$ at 25 °C.** The principle counterion in the previous two subsections is $Na^+$, and it is also worthwhile to consider how well the procedure works for divalent ions which provide a more severe test of the continuum primitive model. There is limited conductance data of FHMA in the presence of $Ca^{2+}$ principle counterion from the work of Vrhovsek et al.[24] and we shall analyze some of their results here using Model A. The values of $pK_1$ and $pK_2$ should be unchanged from before (1.8 and 4.2, respectively), but $pK_B$ is expected to be different. In the experiment, FHMA samples of variable concentration are titrated with $Ca(OH)_2$ until the pH reaches 6.0 and the molar conductance ($\Lambda = \kappa/c = \kappa/(12c_x)$) is plotted versus $c^{1/2}$. The experimental curve (diamonds) and Model A results (lines) for variable $pK_B$ are plotted in Figure 5 at $T$ = 25 °C. Good fit to

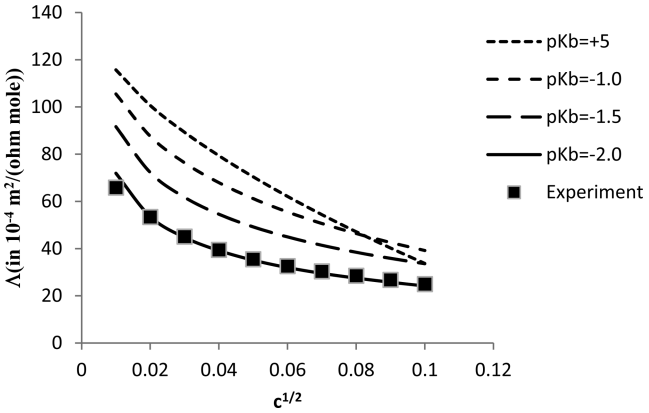


**Figure 5.** ) Equivalent Conductance, Λ (in $10^{-4}$ $m^2$/(ohm mole)) of FHMA versus $c$ for Model A and experiment at pH = 6 and 25 °C, where the counterion is $Ca^{+2}$. Experimental data comes from Vrhovsek et al.[24] Lines are the result of modeling with $pK_1$ = 1.8, $pK_2$ = 4.2, and variable $pK_B$.

experimental data is achieved for $pK_B$ = −2. As in the case of $Na^+$, it is necessary to include some degree of counterion binding in order to reconcile experimental and model conductances. Similar fits are also achieved at 5, 15, and 35 °C.

**3.4. Distributions of FHMA Species with pH.** Although the conductance and titration behavior measured experimentally does not provide direct evidence of the charge state of the FHMA particles and details about specific counterion binding, the model developed in this work allows us to investigate this issue, and we shall illustrate this with Model A in the presence of $Na^+$ (principal counterion) at 25 °C with $pK_1$ = 1.8, $pK_2$ = 4.2, $pK_B$ = −1.4. These parameters were deduced in Subsection 3.2. In the absence of counterion binding ($pK_B$ = +5), the distribution of valence charge of FHMA versus pH exhibits the behavior expected of a polyprotic acid. However, specific binding alters this distribution. Shown in Figure 6 are the fractional distributions of FHMA model particles with valence charges of −6 through −10. Other species may also be present, but in lower concentration. At high pH, the dominant species carries a valence charge of −9 with lesser quantities of −7, −8, and −10 species. It should be emphasized, however, that the model predicts a range of different charge species present at a particular pH, and this distribution changes with pH. Also shown on Figure 6 is the average number of bound $Na^+$ divided by 3.243 (the average number bound at pH = 9.85). Below a

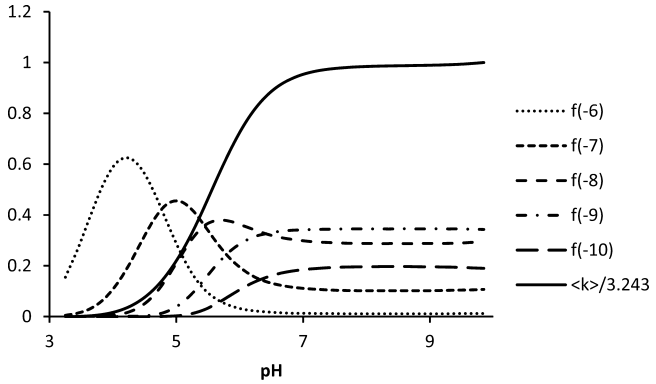


**Figure 6.** Ion charge distributions and extent of counterion binding in model FHMA. The model is Model A described in the text with $pK_1$, $pK_2$, and $pK_B$ equal to 1.8, 4.2, and −1.4, respectively at 25 °C, $c_x$ = $1.15 \times 10^{-4}$ M. The various dotted curves give the fraction of FHMA particles in the designated net charge states of −6 through −10 as a function of pH. Other charge states are present, but in only a small amount. The solid line represents the average number of bound $Na^+$ ions divided by 3.243. The average number of bound $Na^+$ ions is 3.243 at pH = 9.85.

pH of 4, very little $Na^+$ is bound. However, the fraction of bound sodium rises sigmoidally with pH and reaches a plateau value at a pH of about 7.

The distributions shown in Figure 6 do not provide information about the number of bound $Na^+$ in the different valence charge states. For example, a valence charge of −9 could be due to $XH_3^{-9}$, $XH_2Na^{-9}$, $XHNa_2^{-9}$, and/or $XNa_3^{-9}$. Define $X(z,k)$ as the fraction of FHMA model species with a valence charge of $z$ that have $k$ specifically bound $Na^+$ ions. For example $X(-9,1)$ is the fraction of the −9 species (due to $XH_3^{-9}$, $XH_2Na^{-9}$, $XHNa_2^{-9}$, and $XNa_3^{-9}$) present as $XH_2Na^{-9}$. Up to a pH of about 5, all −9 charged species are present as $XH_3^{-9}$ and above a pH of about 7, as $XNa_3^{-9}$. In the mid pH range of 5 to 7, substantial fractions of $XH_2Na^{-9}$ and $XHNa_2^{-9}$ are also present.

## 4. DISCUSSION

The overall objective of the present work is to determine how well the coarse-grained continuum primitive model can account for the titration and conductance behavior of a small, well characterized, prototypical polyelectrolyte. The system we chose to analyze is a derivative of fullerene containing six malonic acid residues covalently attached to the $C_{60}$ core, FHMA. As discussed in Section 2 and the Supporting Information, the principal input parameters are the intrinsic $pK$'s of the two carboxylic acid groups of malonic acid, $pK_1$ and $pK_2$, the net number of charge sites present, $n$, the specific binding constant of a principle counterion, $pK_B$, the hydrodynamic radius of the particle, $a$, the distance of the fixed charges of the particle from its center, $b$, temperature, $T$, solvent viscosity, $\eta$, dielectric properties of the particle and fluid, and properties of the principal counterion, $A^{+z}$. Electrostatics are solved numerically at the level of the nonlinear Poisson−Boltzmann equation and account is also taken of the influence electrostatics has on the various dissociation states of the particle. From these input parameters, the concentrations of various charge states and binding states (of $A^{+z}$) are determined, and this allows us to construct the titration curve ($\alpha_n$ versus pH) of the model particle and compare it with experiment. In order to predict the electrical conductance,[14] it


dx.doi.org/10.1021/jp500196j | J. Phys. Chem. B 2014, 118, 3150−3155

is necessary to determine the electrophoretic mobilities of the various charge states of the model FHMA particle and this is done using the O'Brien and White procedure.[29] The contribution to the conductance of the small ions is estimated using a procedure based on the Onsager–Fuoss procedure.[4,14]

## 5. CONCLUDING REMARKS

For reasonable choices of input parameters, we have been able to obtain good agreement between modeling and experiment for both titration and conductance data. However, it is necessary to include specific binding of the principal counterion in order to achieve this and this necessity is quite striking. This is true not only for $Na^+$, but for $Ca^{2+}$ as well. It should be emphasized that other explanations are possible. Cerar and Skerjanc[32] interpreted the conductance/titration data of FHMA in alkali and calcium salts in terms of a widely used two state model developed many years ago by Wall and co-workers.[33] On the basis of this model, it was determined that the fraction of "free" and "bound" counterions in the presence of FHMA is roughly the same for $Li^+$, $Na^+$, and $Cs^+$ and concluded that counterion association with FHMA is largely electrostatic in nature. In the modeling carried out in the present work, electrostatic association at the level of the (nonlinear) Poisson–Boltzmann equation is not regarded as "binding" so the terms have different meanings in different modeling strategies. Nonetheless, the work of Cerar and Skerjanc[32] indicates that our modeling would reveal comparable "specific binding" of all alkali ions and that indeed is the case. In light of this, we are currently exploring alternative explanations to specific binding. One possibility is that the mobility of counterions that are in close proximity to FHMA are lower than bulk values due to hydrodynamic interaction, HI[34] and the results of that study will hopefully be reported in future work. We believe that the results presented here will stimulate new interest in applying coarse-grained modeling strategies to more complicated systems in chemical engineering, chemistry, nanoscience, and molecular biology. In addition to modeling experimental observables such as titration behavior and electrical conductance, it is possible to also use modeling to investigate other issues such as the distribution of charge and binding states of the model particles.

## ■ ASSOCIATED CONTENT

### Supporting Information

Preliminary model and conservancy relations, Concentrations of Particle Species, Poisson–Boltzmann equation and algorithm to determine particle concentrations, electrophoretic mobility and conductance of complex aqueous solutions., and FHMA continuum model. This material is available free of charge via the Internet at http://pubs.acs.org.

## ■ AUTHOR INFORMATION

### Corresponding Author

*E-mail: sallison@gsu.edu; phone: 404-413-5586; fax: 404-413-5505.

### Notes

The authors declare no competing financial interest.

## ■ REFERENCES

(1) Fuoss, R. M. Paired Ions: Dipolar Pairs as Subset of Diffusion Pairs. *J. Phys. Chem.* **1978**, *82*, 2427–2440.
(2) Huckel, E. The Cataphoresis of the Sphere. *Phys. Z.* **1924**, *25*, 204–210.
(3) Onsager, L. The Theory of Electrolytes. *Phys. Z.* **1926**, *26*, 382–392.
(4) Onsager, L.; Fuoss, R. M. Irreversible Processes in Electrolytes. Diffusion, Conductance and Viscous Flow in Arbitrary Mixtures of Strong Electrolytes. *J. Phys. Chem.* **1932**, *36*, 2689–2778.
(5) Pitts, E. An Extension of the Theory of Conductivity and Viscosity of Electrolyte Solutions. *Proc. R. Soc. London, Ser. A* **1953**, *217*, 43–70.
(6) Fuoss, R. M.; Onsager, L. Conductance of Strong Electrolytes at Finite Dilutions. *Proc. Natl. Acad. Sci. U. S. A.* **1955**, *41*, 274–283.
(7) Fuoss, R. M.; Onsager, L. Conductance of Unassociated Electrolytes. *J. Phys. Chem.* **1957**, *61*, 668–682.
(8) Fuoss, R. M.; Hsia, K.-L. Association of 1–1 Salts in Water. *Proc. Natl. Acad. Sci. U. S. A.* **1967**, *57*, 1550–1557.
(9) Quint, J.; Viallard, A. Electrical Conductance of Electrolyte Mixtures of Any Type. *J. Solution Chem.* **1978**, *7*, 533–548.
(10) Justice, J.-C.; Ebeling, W. Ionic Interactions in Solutions. IV. Conductance Theory of Binary Electrolytes for Hamiltonian Models. *J. Solution Chem.* **1979**, *8*, 809–833.
(11) Bianchi, H.; Fernandez-Prini, R. The Conductivity of Dilute Electrolyte Solutions: Expanded Lee and Wheaton Equation for Symmetrical, Unsymmetrical, and Mixed Electrolytes. *J. Solution Chem.* **1993**, *22*, 557–570.
(12) Tomsic, M.; Bester-Rogac, M.; Jamnik, A.; Neueder, R.; Barthel, J. Conductivity of Magnesium Sulfate in Water from 5 to 35 °C and from Infinite Dilution to Saturation. *J. Solution Chem.* **2002**, *31*, 19–31.
(13) Bester-Rogac, M.; Babic, V.; Perger, T. M.; Neueder, R.; Barthel, J. Conductometric Study of Ion Association in Divalent Symmetric Electrolytes: I. $CoSO_4$, $NiSO_4$, $CuSO_4$, and $ZnSO_4$ in Water. *J. Mol. Liq.* **2005**, *118*, 111–118.
(14) Allison, S. A.; Wu, H.; Twahir, U.; Pei, H. Conductivity and Electrophoretic Mobility of Dilute Ionic Solutions. *J. Colloid Interface Sci.* **2010**, *352*, 1–10.
(15) Kroto, H. W.; Heath, J. R.; Obrien, S. C.; Curl, R. F.; Smalley, R. E. $C_{60}$: Buckminsterfullerene. *Nature* **1985**, *318*, 162–163.
(16) Noon, W. H.; Kong, Y. F.; Ma, J. P. Molecular Dynamics Analysis of a Buckyball-Antibody Complex. *Proc. Natl. Acad. Sci. U. S. A.* **2002**, *99*, 6466–6470.
(17) Zakharian, T. Y.; Seryshev, A.; Sitharaman, B.; Gilbert, B. E.; Knight, V.; Wilson, L. J.; Fullerene-Paclitaxel Chemotherapeutic, A. Synthesis, Characterization, and Study of Biological Activity in Tissue Culture. *J. Am. Chem. Soc.* **2005**, *127*, 12508–12509.
(18) King, R. B. Chemical Structure and Superconductivity. *J. Chem. Inf. Comput. Sci.* **1999**, *39*, 180–191.
(19) Sun, Y. P.; Riggs, J. E.; Liu, B. Optical Limiting Properties of [60] Fullerene Derivatives. *Chem. Mater.* **1997**, *9*, 1268–1272.
(20) Haddon, R. C. C60: Sphere or Polyhedron? *J. Am. Chem. Soc.* **1997**, *119*, 1797–1798.
(21) Kato, T.; Kikuchi, K.; Achiba, Y. Measurement of the Self-Diffusion Coefficient of $C_{60}$ in Benzene-$d_6$ Using $^{13}C$ Pulsed-Gradient Spin Echo. *J. Phys. Chem.* **1993**, *97*, 10251–10253.
(22) Cerar, J.; Cerkovnik, J.; Skerjanc, J. Water-Soluble Fullerenes. 1. Fullerenehexamalonic Acid $T_h$-$C_{66}(COOH)_{12}$, an Intermediate Spherical Electrolyte. *J. Phys. Chem. B* **1998**, *102*, 7377–7381.
(23) Cerar, J.; Skerjanc, J. Water-Soluble Fullerenes. 2. Fullerenehexamalonate $T_h$-$C_{66}(COONa)_{12}$, a Highly Asymmetric Electrolyte. *J. Phys. Chem. B* **2000**, *104*, 727–730.
(24) Vrhovsek, A.; Cerar, J.; Bester-Rogac, M.; Skerjanc, J. Effect of Temperature on the Molar Conductivity of Aqueous Solutions of Sodium and Calcium Fullerenehexamalonates, $T_h$-$C_{66}(COONa)_{12}$ and $T_h$-$C_{66}((COO)_2NCa)_6$. *Phys. Chem. Chem. Phys.* **2001**, *3*, 2650–2654.
(25) Henry, D. C. The Cataphoresis of Suspended Particles. Part 1. The Equation of Cataphoresis. *Proc. R. Soc. London, Ser. A* **1931**, *133*, 106–129.
(26) Overbeek, J. Th. G. Theory of Electrophoresis. The Relaxation Effect. *Kolloid-Beih.* **1943**, *54*, 87–364.
(27) Booth, F. The Cataphoresis of Spherical Particles in Strong Fields. *Proc. R. Soc. London, Ser. A* **1950**, *203*, 514–551.

(28) Wiersema, P. H.; Loeb, A. L.; Overbeek, J.; Th, G. Calculation of the Electrophoretic Mobility of a Spherical Colloid Particle. *J. Colloid Interface Sci.* **1966**, *22*, 78−99.
(29) O'Brien, R. W.; White, L. R. Electrophoretic Mobility of a Spherical Colloid Particle. *J. Chem. Soc., Faraday Trans. 2* **1978**, *74*, 1607−1626.
(30) Ma, Y.; Zhu, C.; Ma, P.; Yu, K. T. Studies of the Diffusion Constants of Amino Acids in Aqueous Solutions. *J. Chem. Eng. Data* **2005**, *50*, 1192−1196.
(31) Edward, J. T. Molecular Volumes and the Stokes−Einstein Equation. *J. Chem. Educ.* **1970**, *47*, 261−270.
(32) Cerar, J.; Skerjanc, J. Electric Transport and Ion Binding in Solutions of Fullerenehexamalonic Acid $T_h$-$C_{66}(COOH)_{12}$ and Its Alkali and Calcium Salts. *J. Phys. Chem. B* **2008**, *112*, 892−895.
(33) Huizenga, J.; Grieger, P.; Wall, F. Electrolytic Properties of Aqueous Solutions of Polyacrylic Acid and Sodium Hydroxide. I. Transference Experiments Using Radioactive Sodium. *J. Am. Chem. Soc.* **1950**, *72*, 2636−2642.
(34) Allison, S. Diffusion-Controlled Reactions: Hydrodynamic Interaction between Charged, Uniformly Reactive Spherical Particles. *J. Phys. Chem. A* **2008**, *112*, 892−895.